

Enhancement of Electronic Spin Susceptibility in Pauli Limited Unconventional Superconductors

Benjamin M. Rosemeyer and Anton B. Vorontsov

Department of Physics, Montana State University, Montana 59717, USA

(Dated: August 25, 2014)

We calculate the wave-vector dependent electronic spin susceptibility $\chi_{\alpha\beta}(\mathbf{q}, \mathbf{H}_0)$ of a superconducting state in uniform magnetic field \mathbf{H}_0 . We consider Pauli-limited superconductivity with d -wave symmetry, and a 2D cylindrical Fermi surface. We find that the transverse component of the susceptibility tensor is enhanced over its normal state value; the longitudinal component also slightly increases but in a very limited range of q -s. We identify several wave vectors $\{\mathbf{q}_\perp, \mathbf{q}_\parallel\}$, that correspond to the maxima of either χ_\perp or χ_\parallel . We compare our results with available data on the high-field phase in heavy-fermion CeCoIn₅.

PACS numbers: 74.20.Rp, 74.25.Ha, 74.70.Tx

Interplay of superconductivity (SC) and magnetism has been an active field of research for many years. Singlet superconductivity is competing with ferromagnetic order which produces strong uniform internal fields and destroys spin-zero Cooper pairs. This competition usually results in suppression of one of the orders. [1] The antiferromagnetic (AFM) order, on the other hand, and interferes much less with superconductivity, as it gives rise to field oscillations on a short atomic scale, much smaller than the Cooper pair size ξ_0 . [2] Moreover, in unconventional superconductors under certain conditions the superconducting and antiferromagnetic spin-density wave (SDW) orders are attractive. [3]

Recent years have seen another cycle of interest in understanding the details of the SC-SDW interactions due to discovery of iron-based superconductors [4] and Ce-family of heavy-fermion materials [5, 6]. In pnictides the co-existence of the SDW and SC is due to the multi-band nature and unconventional order parameter structure. The interplay of two orders is a strong function of the Fermi surface (FS) topology. [7] In heavy-fermion Pauli-limited CeCoIn₅ the normal state is non-magnetic but the SDW magnetism appears in the high-field low-temperature part of the phase diagram, through a second-order transition, and disappears simultaneously with superconductivity at first-order H_{c2} transition, see Fig. 1. [6, 8, 9] The experiments point towards strong AFM fluctuations in the normal state, [10] which, however, are not strong enough to produce SDW instability. Nonetheless, these fluctuations can be enhanced by doping, [11] or possibly by magnetic field, and result in AFM order.

Following the initial suggestion that the anomalous phase could be a non-uniform Fulde-Ferrell-Larkin-Ovchinnikov (FFLO) state, [12] several theories appeared that connected the onset of magnetic order to the density of states enhancement by spatially non-uniform SC states, including FFLO [13, 14] and vortex cores. [15]. There is, however, still no direct evidence of the FFLO state in this material.

Another recently proposed mechanism is based on the interaction of the uniform superconducting state with magnetic field, when Pauli depairing produces favorable conditions for AFM instability inside the SC phase. [16] The mechanism behind this effect was further revealed in [17], which connected the emerging AFM instability with the appearance of spin-polarized quasiparticle pockets near gap nodes, and “nesting” of those pockets in momentum space.

The details of this “attraction” between SDW order and Pauli-suppressed SC are still not fully uncovered. All theories so far assumed only single direction of the SDW ordering vector \mathbf{q} , connecting nodes, independent of temperature and the field. The size of the SDW phase has not been explicitly connected with the microscopic parameters such as size of the SC gap, band width or Fermi energy, and strength of the magnetic interactions.

In this paper we present a microscopic picture of the SDW instability in unconventional d -superconductors, and find several key features consistent with the experiments on CeCoIn₅. We calculate the spin susceptibility as a function of magnetization ordering vector \mathbf{q} , temperature and field, and determine onset of the magnetic instability in the phase diagram. Susceptibility gives detailed information about possible ordering vectors, direction of magnetization, and their variation with field and temperature. Its magnitude relates the size of the SDW region to magnetic interaction strength, SC gap (low) and band (high) energy scales. We determine how the ordering vectors at instability change with field and temperature. We find that the mechanism behind enhancement lies not in near-perfect “nesting” of quasiparticle pockets, but rather in combination of the dispersion of the new quasiparticles, phase space and the structure of the order parameter. At high fields there are multiple \mathbf{q} vectors connecting the sharp end of the pockets. Such flexibility offers robustness of the SDW instability against orbital effects.

Our model is a mean-field SC Hamiltonian with 2D cylindrical FS, and electrons interacting with uniform

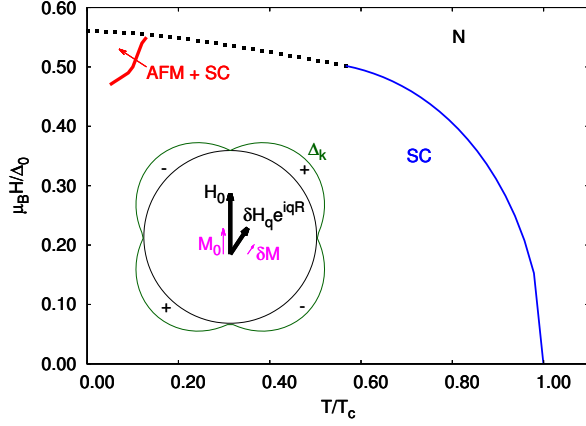


FIG. 1. (Color online) Phase diagram of Pauli-limited superconductor, with the co-existence state shown. Insert: we consider circular Fermi surface, and d -wave order parameter $\Delta_{\mathbf{k}} = \Delta_0(T, H) \sin 2\phi_{\mathbf{k}}$. The magnetic field has large uniform component \mathbf{H}_0 and spatially varying perturbation $\delta\mathbf{H}_{\mathbf{q}}$ with wave vector \mathbf{q} .

magnetic field \mathbf{H}_0 through Zeeman term: $\mathcal{H} = \mathcal{H}_0 + V$

$$\mathcal{H}_0 = \sum_{\mathbf{k}\mu} \xi_{\mathbf{k}} c_{\mathbf{k}\mu}^\dagger c_{\mathbf{k}\mu} + \sum_{\mathbf{k}} \left(\Delta_{\mathbf{k}} c_{\mathbf{k}\uparrow}^\dagger c_{-\mathbf{k}\downarrow}^\dagger + h.c. \right) + \mu_B \sum_{\mathbf{k}\mu\nu} c_{\mathbf{k}\mu}^\dagger \boldsymbol{\sigma}_{\mu\nu} \mathbf{H}_0 c_{\mathbf{k}\nu} \quad (1)$$

and for linear response we include a \mathbf{q} -dependent perturbation of the magnetic field $\delta\mathbf{H}(\mathbf{R}) = \delta\mathbf{H}_{\mathbf{q}} e^{i\mathbf{q}\cdot\mathbf{R}}$, $V = \mu_B \sum_{\mathbf{k}\mu\nu} c_{\mathbf{k}+\mathbf{q}\mu}^\dagger \boldsymbol{\sigma}_{\mu\nu} \delta\mathbf{H}_{\mathbf{q}} c_{\mathbf{k}\nu}$, where μ_B is the mag-

netic moment of electron. The electronic dispersion in the normal state is $\xi_{\mathbf{k}} = \frac{\mathbf{k}^2}{2m^*} - \epsilon_F$. The resulting magnetization has uniform part and \mathbf{q} -dependent perturbation:

$$M_{\alpha}(\mathbf{R}) = M_{0\alpha}(\mathbf{H}_0) + \chi_{\alpha\beta}(\mathbf{q}) \delta H_{\beta} e^{i\mathbf{q}\cdot\mathbf{R}} \quad (2)$$

with $\mathbf{M}_0(\mathbf{r}, t) = \mu_B \langle \mathbf{S}(\mathbf{r}, t) \rangle_0$, and susceptibility [18]:

$$\chi_{\alpha\beta}(\mathbf{r}, t) = \frac{i\mu_B^2}{\hbar} \langle [S_{\alpha}(\mathbf{r}, t), S_{\beta}(0, 0)] \theta(t) \rangle_0$$

$$\chi_{\alpha\beta}(\mathbf{q}) = \int d^3r e^{-i\mathbf{q}\cdot\mathbf{r}} \int_0^{\infty} dt e^{-0^+ t} \chi(\mathbf{r}, t) \quad (3)$$

where $\mathbf{S}(\mathbf{r}, t) = \sum_{\mu\nu} \psi_{\mu}^\dagger(\mathbf{r}, t) \boldsymbol{\sigma}_{\mu\nu} \psi_{\nu}(\mathbf{r}, t)$, $\psi_{\nu}(\mathbf{r}, t) = \sum_{\mathbf{k}} c_{\mathbf{k}\nu}(t) \varphi_{\nu}(\mathbf{r})$, $c_{\mathbf{k}\nu}(t) = e^{i\mathcal{H}_0 t} c_{\mathbf{k}\mu} e^{-i\mathcal{H}_0 t}$; subscript 0 indicates the average over ensemble (1).

The temperature and magnetic field dependence of the uniform magnetization \mathbf{M}_0 is known, e.g.[19] and here we discuss the susceptibility $\chi_{\alpha\beta}(\mathbf{q})$, since it determines the magnetic instability into an SDW state, and the RKKY-type interaction between localized moments. We diagonalize Hamiltonian (1) by the Bogoliubov transformation, $c_{\mathbf{k}\mu} = u_{\mathbf{k}} \gamma_{\mathbf{k}\mu} + (i\sigma_2)_{\mu\nu} v_{\mathbf{k}}^* \gamma_{-\mathbf{k}\nu}^\dagger$ with spin-independent coefficients,

$$u_{\mathbf{k}} = \sqrt{\frac{1}{2} \left(1 + \frac{\xi_{\mathbf{k}}}{\epsilon_{\mathbf{k}}} \right)}, \quad v_{\mathbf{k}} = \text{sgn}(\Delta_{\mathbf{k}}) \sqrt{\frac{1}{2} \left(1 - \frac{\xi_{\mathbf{k}}}{\epsilon_{\mathbf{k}}} \right)}, \quad (4)$$

(here $\epsilon_{\mathbf{k}} = \sqrt{\xi_{\mathbf{k}}^2 + \Delta_{\mathbf{k}}^2}$) which results in new quasiparticle spectrum $\mathcal{H}_0 = \sum_{\mathbf{k}\mu} \epsilon_{\mathbf{k}\mu} \gamma_{\mathbf{k}\mu}^\dagger \gamma_{\mathbf{k}\mu}$, with $\epsilon_{\mathbf{k}\mu} = \epsilon_{\mathbf{k}} \pm \mu_B H_0$.

Using these expressions in (3), the general formulas for longitudinal ($\delta\mathbf{M} = \chi_{\parallel} \delta\mathbf{H} \parallel \mathbf{H}_0$) and transverse ($\delta\mathbf{M} = \chi_{\perp} \delta\mathbf{H} \perp \mathbf{H}_0$) components of the susceptibility tensor are:

$$\chi_{\parallel}(\mathbf{q}) = -\mu_B^2 \sum_{\mathbf{k}\mu} \left\{ \frac{[f(\epsilon_{\mathbf{k}-\mu}) - f(\epsilon_{\mathbf{k}+\mu})](u_{\mathbf{k}+} u_{\mathbf{k}-} + v_{\mathbf{k}+} v_{\mathbf{k}-})^2}{\epsilon_{\mathbf{k}-\mu} - \epsilon_{\mathbf{k}+\mu}} - \frac{[1 - f(\epsilon_{\mathbf{k}-\mu}) - f(\epsilon_{\mathbf{k}+\mu})](u_{\mathbf{k}+} v_{\mathbf{k}-} - v_{\mathbf{k}+} u_{\mathbf{k}-})^2}{\epsilon_{\mathbf{k}-\mu} + \epsilon_{\mathbf{k}+\mu}} \right\} \quad (5a)$$

$$\chi_{\perp}(\mathbf{q}) = -\mu_B^2 \sum_{\mathbf{k}\mu} \left\{ \frac{[f(\epsilon_{\mathbf{k}-\mu}) - f(\epsilon_{\mathbf{k}+\mu})](u_{\mathbf{k}+} u_{\mathbf{k}-} + v_{\mathbf{k}+} v_{\mathbf{k}-})^2}{\epsilon_{\mathbf{k}-\mu} - \epsilon_{\mathbf{k}+\mu}} - \frac{[1 - f(\epsilon_{\mathbf{k}-\mu}) - f(\epsilon_{\mathbf{k}+\mu})](u_{\mathbf{k}+} v_{\mathbf{k}-} - v_{\mathbf{k}+} u_{\mathbf{k}-})^2}{\epsilon_{\mathbf{k}-\mu} + \epsilon_{\mathbf{k}+\mu}} \right\} \quad (5b)$$

where $f(\epsilon) = [\exp(\epsilon/T) + 1]^{-1}$ is the Fermi distribution, and momenta are shifted by the magnetization wave vector $\mathbf{k}_{\pm} = \mathbf{k} \pm \mathbf{q}/2$. Notation $\bar{\mu}$ means spin state opposite to $\mu = \pm 1$.

In the normal state ($\Delta_{\mathbf{k}} = 0$), one obtains the familiar

Lindhard function,

$$\chi_{\parallel}^N(\mathbf{q}) = -\mu_B^2 \sum_{\mathbf{k}\mu} \frac{f(\xi_{\mathbf{k}\mu}) - f(\xi_{\mathbf{k}+\mathbf{q}\mu})}{\xi_{\mathbf{k}\mu} - \xi_{\mathbf{k}+\mathbf{q}\mu}} \quad (6)$$

$$\chi_{\perp}^N(\mathbf{q}) = -\mu_B^2 \sum_{\mathbf{k}\mu} \frac{f(\xi_{\mathbf{k}\mu}) - f(\xi_{\mathbf{k}+\mathbf{q}\bar{\mu}})}{\xi_{\mathbf{k}\mu} - \xi_{\mathbf{k}+\mathbf{q}\bar{\mu}}}$$

where $\xi_{\mathbf{k}\mu} = \frac{k^2}{2m^*} - \epsilon_F \pm \mu_B H_0$ are electron excitation energies in magnetic field. At zero temperature the Fermi functions are step-functions, and the integration over mo-

menta can be done analytically; in two dimensions we get

$$\frac{\chi_{\parallel}^N(q)}{\chi_0} = 1 - \frac{1}{2}\theta(q - 2k_{f\uparrow})\sqrt{1 - \left(\frac{2k_{f\uparrow}}{q}\right)^2} - \frac{1}{2}\theta(q - 2k_{f\downarrow})\sqrt{1 - \left(\frac{2k_{f\downarrow}}{q}\right)^2} \quad (7)$$

$$\frac{\chi_{\perp}^N(q)}{\chi_0} = 1 - \frac{1}{2}\theta(q - k_{f\uparrow} - k_{f\downarrow}) \left[\sqrt{\left(1 + \frac{k_{f\uparrow}^2 - k_{f\downarrow}^2}{q^2}\right)^2 - \left(\frac{2k_{f\uparrow}}{q}\right)^2} + \sqrt{\left(1 + \frac{k_{f\downarrow}^2 - k_{f\uparrow}^2}{q^2}\right)^2 - \left(\frac{2k_{f\downarrow}}{q}\right)^2} \right] \quad (8)$$

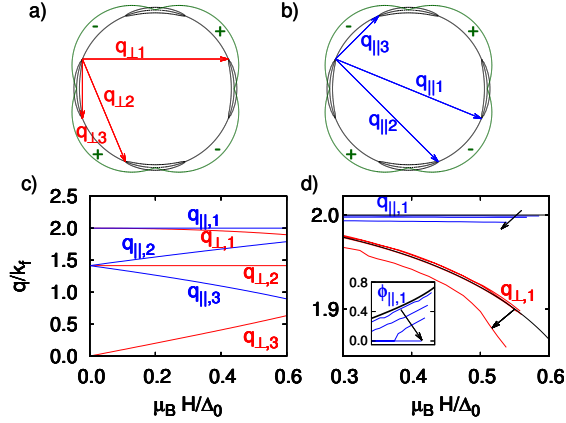


FIG. 2. (Color online) (a,b) Magnetic field produces pockets of low energy spin-down excitations near the nodes of the d-wave order parameter. The largest enhancement of χ_{\perp} susceptibility occurs when magnetic ordering vector connects ends of quasiparticle pockets with opposite sign gap (a), or ends with the same sign gap for χ_{\parallel} (b). (c) The magnitude of the ordering vectors as a function of the field at zero temperature, from (a,b). (d) Finite temperature effects, from $T = 0$ to $T = 0.3T_c$ shown by arrows, on $q_{\parallel,\perp 1}$ vectors, and angle $\phi_{\parallel 1}$ between $\mathbf{q}_{\parallel 1}$ and x-axis (inset).

Here $\chi_0 = 2\mu_B^2 N_F$ is Pauli susceptibility at $q = 0$, and $k_{f\uparrow\downarrow}^2 = k_f^2(1 \mp \mu_B H_0/\epsilon_F)$ are the Fermi momenta for two spin projections. The parallel component shows two kinks, at $q = 2k_{f\uparrow}$ and $2k_{f\downarrow}$, when the Fermi surfaces of up- and down-spins touch at a single point, whereas transverse component involves opposite spins which results in only one kink at $q = k_{f\uparrow} + k_{f\downarrow}$. Generally, the value and behavior of $\chi(q)$ is determined by the properties of the dispersion $\xi_{\mathbf{k}}$ at hot spots, where $\xi_{\mathbf{k}+\mathbf{q}} = -\xi_{\mathbf{k}}$. Near those spots both denominator and numerator in χ are close to zero, and the value of the susceptibility is determined by the phase space, which is a function of \mathbf{k} -space dimensionality and the shape of the Fermi surface. For example, in one dimensional case or for Fermi surfaces with flat parts the susceptibility is logarithmically divergent. [20]

In the superconducting *d*-wave state we want to find the maximal values of susceptibility and the correspond-

ing magnetization wave vectors. Nodal regions of $\Delta_{\mathbf{k}}$ allow spin-down quasiparticles with negative energies, which form new Fermi surface pockets,[17] and partially destroy superconductivity. In the $\mathbf{q} \rightarrow 0$ limit these quasiparticles result in finite $\chi_{\parallel}(0)/\chi_0 \sim \mu_B H_0/\Delta_0$. However, the opposite spin coupling in the first term of (5b) ensures $\chi_{\perp}(0) = 0$.

Analytic analysis of Eqs. (5) in general is quite difficult, and the result will strongly depend on the topology of the Fermi surface, field and temperature. However, the important factors to find the vectors \mathbf{q} that maximize the susceptibility can be stated in $T = 0$ limit. These vectors are shown in Fig. 2(a),(b) for χ_{\perp} and χ_{\parallel} , and they connect the sharp ends of the spin-down quasiparticle pockets, given by $\epsilon_{\mathbf{k}\downarrow} = \sqrt{\xi_{\mathbf{k}}^2 + \Delta_{\mathbf{k}}^2} - \mu_B H = 0$. This result is in accord with the enhanced quasiparticle scattering with similar vectors observed in [21]. In the vicinity of such common point, $\epsilon_{\mathbf{k}\pm\downarrow} \approx \epsilon_{\mathbf{k}\downarrow} \approx 0$ and the denominators of the first (second) term in longitudinal χ_{\parallel} , (transverse χ_{\perp}) response, can be expanded as $\mathbf{v}_+\delta\mathbf{k} + \mathbf{v}_-\delta\mathbf{k}$, in regions allowed by the distribution functions in numerators. The contribution to χ is greatest when the group velocities $\mathbf{v}_{\pm} = \nabla_{\mathbf{k}}\epsilon_{\mathbf{k}\pm\downarrow}$ are the smallest, *i.e.* near the sharp ends of the banana-like regions, where quasiparticle velocity is related to the opening rate of the gap $v_{\Delta} = \partial\sqrt{v_F^2 k_{\perp}^2 + \Delta_0^2 \sin^2 2\phi}/\partial(k_F\phi) \sim v_F(\Delta_0/\epsilon_F) \ll v_F$. The actual magnitude of χ is determined by the available phase space given by complicated FS overlap in 2D \mathbf{k} -plane, and the superconducting coherence factors. The longitudinal first term is maximized when the magnetization vector \mathbf{q} connects the same $\Delta_{\mathbf{k}}$ -sign points, making $(u_{\mathbf{k}_+}u_{\mathbf{k}_-} + v_{\mathbf{k}_+}v_{\mathbf{k}_-})$ the most positive and largest with $v_{\mathbf{k}_+}v_{\mathbf{k}_-} > 0$; similarly, largest χ_{\perp} is reached when $(u_{\mathbf{k}_+}v_{\mathbf{k}_-} - v_{\mathbf{k}_+}u_{\mathbf{k}_-})$ is the most positive. This occurs at vectors, connecting points with opposite signs of $\Delta_{\mathbf{k}\pm}$. The length of the magnetic vectors at $T = 0$ is shown in Fig. 2(c) as function of magnetic field.

We confirm this analysis and further investigate dependence on the temperature and field, $T \sim \mu_B H_0 \sim \Delta_0 \ll \epsilon_F$ numerically. In Fig. 2(d) we show the T -induced deviations of optimal \mathbf{q}_1 vectors from their $T = 0$ values. At each T and H_0 we self-consistently compute the amplitude of the gap function $\Delta_{\mathbf{k}} = \Delta(T, H) \sin 2\phi_{\mathbf{k}}$

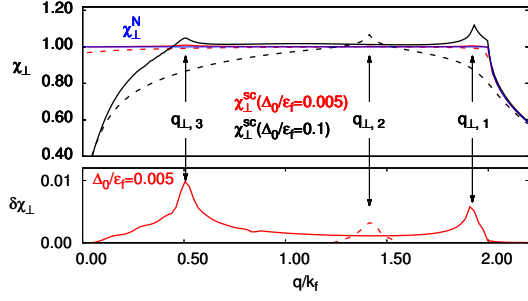


FIG. 3. (Color online) The $T = 0$ normalized susceptibility in the superconducting (red) and normal states (blue) as a function of q . We set $\mu_B H = 0.5\Delta_0$, close to the Pauli limiting field $\mu_B H_P/\Delta_0 = 0.56$, and $\Delta_0/\epsilon_F = 0.005$. Transverse susceptibility shows enhancement over the normal state $\chi^N(q)$ with 2 peaks at $q_{\perp 1,3}$ for nodal- \mathbf{q} direction (solid), and one peak for $\mathbf{q} \parallel \mathbf{q}_{\perp 2}$ (dashed), in accordance with Fig. 2(a,c). The lower pane shows $\delta\chi_{\perp}(q) = \chi_{\perp}^{sc}(q) - \chi_{\perp}^N(q)$. The maximal enhancement $\delta\chi_{\perp}(q)$ occurs at wave vectors $\mathbf{q}_{\perp 3,1}$ and is of the order $\delta\chi_{\perp}/\chi_0 \sim \Delta_0/\epsilon_F$.

($\Delta(0,0) = \Delta_0$), which we substitute into Eq. (5). Then we scan over 2D \mathbf{q} vector to locate the maximum of the susceptibility $\chi(\mathbf{q}_{max})$. We find that the ordering vector $\mathbf{q}_{\perp 1}$ in transverse susceptibility is reduced with temperature, resulting in smaller overlap of the quasiparticle pockets. Conversely, for longitudinal component the overlap is increasing with temperature, as seen in the inset from the smaller $\phi_{q\parallel}$ angle.

In Fig. 3 we plot $\chi_{\perp}(q)$ in superconducting state at $T = 0$ and magnetic field $\mu_B H = 0.5\Delta_0$. The directions of the ordering vectors \mathbf{q} are chosen either along nodal line or along $\mathbf{q}_{\perp 2}$ for this field, see Fig. 2(a). For the chosen small value of $\Delta_0/\epsilon_F = 0.005$, the maximal enhancement of χ_{\perp} occurs at the shortest vector q_3 , but we find that the maximum shifts to q_1 vector if $\Delta_0/\epsilon_F \sim 0.1$.

In Fig. 4 we present the T - H phase diagram of a Pauli-limited d -wave superconductor, and plot contours of constant value of the χ_{\perp} peaks, corresponding to different wave vectors $q_{\perp i}$. While in the most part of the phase diagram $\chi_{\perp}^{sc}(q)$ is smaller than the normal state χ^N , in the low T , high H corner (shown) $\delta\chi = \chi_{\perp}^{sc} - \chi_{\perp}^N$ becomes positive and progressively larger. The typical size of the enhancement over the normal state is $\delta\chi/\chi_0 \sim \Delta_0/\epsilon_F$. The contours of enhanced susceptibility $\delta\chi(T, H)$ will determine the boundary of the SDW state inside the uniform SC phase, if the magnetic interaction is strong enough to cause divergence of $\chi_{\alpha\beta}^{RPA}(\mathbf{q}) = \chi_{\alpha\beta}(\mathbf{q})/[1 - J(\mathbf{q})\chi_{\alpha\beta}(\mathbf{q})]$, which may happen in case of strong magnetic fluctuations in the normal state, $J(\mathbf{q})\chi_0 \lesssim 1$.

We note that the longitudinal susceptibility does not show similar enhancement. We find that for $q_{\parallel 1} \sim 2k_F$ the enhancement $\chi_{\parallel}(\mathbf{q}, H_0) > \chi_{\parallel}^N(\mathbf{q}, \mathbf{H}_0)$ can be significant but it occurs on the background of fast-decreasing

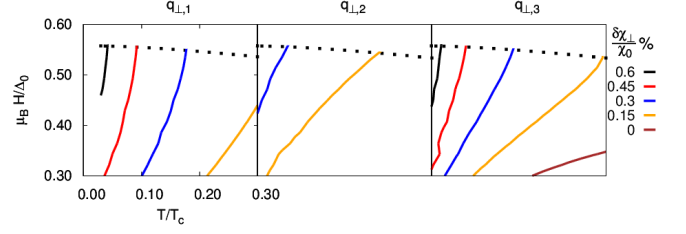


FIG. 4. (Color online) Contour lines of maximal enhancement of transverse susceptibility χ_{\perp} in the T - H phase diagram for $\Delta_0 = 0.005\epsilon_F$. Different contours correspond to relative enhancements $\delta\chi(q)/\chi_0$ given in percents. The three panels correspond to \mathbf{q} -vectors in Fig. 2(a). The dotted line is the first order Pauli-limiting phase transition.

normal state $\chi_{\parallel}^N(\mathbf{q})$ and does not lead to increase over χ_0 .

These results align very well with the experimental data for CeCoIn₅. The general location in the T - H phase diagram and the shape of the SDW instability, determined by enhancement $\delta\chi_{\perp}$, is consistent with the Q-phase transition, and agrees with the conclusions of [17]. The SC-induced enhancement of χ_{\perp} , and absence of such in χ_{\parallel} , explains why the Q-phase is observed only when the H_0 -field is in the ab -plane, and the SDW magnetization is orthogonal to it. We find several possible candidates for the SDW ordering vector \mathbf{q} , only one of which is probably selected by the magnetic interaction $J(\mathbf{q})$. The nodal $\mathbf{q}_{\perp 1}$ is the most likely candidate from experimental point of view which sees ordering at $[0.44, 0.44]\pi/a$ [9] (our gap is 45°-rotated) and it also agrees with the size of the α -FS pocket of CeCoIn₅. [15] The length of this vector drops by about a percent over the $0 - 0.3T_c$ range, and this reduction rate is comparable to change of 0.2% observed in [9] when temperature was changed from 60 mK ($0.025T_c$) to 150 mK ($0.06T_c$). The magnitude of enhancement needed to achieve material parameters. For the ratio $\Delta_0/\epsilon_F \sim 0.6\text{meV}/0.5\text{eV} \sim 0.001$ [22, 23] we found typical enhancement is of about same size $\delta\chi_{\perp}/\chi_0 \sim \Delta_0/\epsilon_F$ i.e. a fraction of a percent. A similar-size enhancement of normal state susceptibility χ_0 can be associated with the FS changes induced by Cd-doping CeCo(In_{1-x}Cd_x)₅. [11, 24, 25] According to their data, doping of $x=0.1$ induces AFM state, and corresponds to 5.5% decrease in FS volume. Linear extrapolation of Neel temperature to zero inside SC state gives 4% minimal doping, that would correspond to a 2% FS decrease, that with a tight-binding dispersion [17] corresponds to 3% increase in χ_0 . Conversely, applying pressure would increase the FS size, reduce χ_0 , and destroy the SDW state. [11]

In conclusion, we investigated the behavior of spin susceptibility in Pauli-limited unconventional superconductors. We found that the field-induced nodal quasiparti-

cles, and the sign-changing nature of the gap, leads to the enhancement of the transverse susceptibility component inside the superconducting phase. We find several magnetic ordering vectors, connecting sharp (high density of states) points of the field-induced Fermi pockets. The enhancement is of the order $\delta\chi/\chi_0 \sim \Delta_0/\epsilon_F$ and is a strong function of temperature and magnetic field; it may result in SDW order formed inside the superconducting phase at low temperatures and high fields, whose features are semi-quantitatively consistent with observations in CeCoIn₅. To get more quantitative agreement with the CeCoIn₅ data one needs to take into account more realistic band structure and 3D topology of the Fermi surface.

This research was done with NSF support through grant DMR-0954342. ABV acknowledges hospitality of Aspen Center for Physics, and discussions with I. Vekhter.

-
- [1] L. N. Bulaevskii, A. I. Buzdin, M. L. Kulić, and S. V. Panjukov, *Advances in Physics* **34**, 175 (1985).
 - [2] P. Anderson and H. Suhl, *Physical Review* **116**, 898 (1959).
 - [3] K. Machida and M. Kato, *Phys. Rev. Lett.* **58**, 1986 (1987); M. Kato and K. Machida, *J Phys Soc Jpn* **56**, 2136 (1987).
 - [4] D. Johnston, *Advances in Physics* **59**, 803 (2010).
 - [5] C. Petrovic, P. G. Pagliuso, M. F. Hundley, R. Movshovich, J. L. Sarrao, J. D. Thompson, Z. Fisk, and P. Monthoux, *Journal of Physics: Condensed Matter* **13**, L337 (2001).
 - [6] M. Kenzelmann, T. Strässle, C. Niedermayer, M. Sigrist, B. Padmanabhan, M. Zolliker, A. D. Bianchi, R. Movshovich, E. D. Bauer, J. L. Sarrao, and J. D. Thompson, *Science* **321**, 1652 (2008).
 - [7] A. B. Vorontsov, M. G. Vavilov, and A. V. Chubukov, *Phys. Rev. B* **81**, 174538 (2010); R. M. Fernandes and J. Schmalian, *ibid.* **82**, 014521 (2010).
 - [8] A. Bianchi, R. Movshovich, C. Capan, P. Pagliuso, and J. Sarrao, *Phys. Rev. Lett.* **91**, 187004 (2003).
 - [9] M. Kenzelmann, S. Gerber, N. Egetenmeyer, J. L. Gavilano, T. Strässle, A. D. Bianchi, E. Ressouche, R. Movshovich, E. D. Bauer, J. L. Sarrao, and J. D. Thompson, *Phys. Rev. Lett.* **104**, 127001 (2010).
 - [10] J. Paglione, M. A. Tanatar, D. G. Hawthorn, E. Boaknin, R. W. Hill, F. Ronning, M. Sutherland, L. Taillefer, C. Petrovic, and P. C. Canfield, *Phys. Rev. Lett.* **91**, 246405 (2003); A. Bianchi, R. Movshovich, I. Vekhter, P. Pagliuso, and J. Sarrao, *ibid.* **91**, 257001 (2003).
 - [11] L. D. Pham, T. Park, S. Maquilon, J. D. Thompson, and Z. Fisk, *Phys. Rev. Lett.* **97**, 056404 (2006); K. Gofryk, F. Ronning, J.-X. Zhu, M. N. Ou, P. H. Tobash, S. S. Stoyko, X. Lu, A. Mar, T. Park, E. D. Bauer, J. D. Thompson, and Z. Fisk, *ibid.* **109**, 186402 (2012).
 - [12] P. Fulde and R. Ferrell, *Phys. Rev.* **135**, A550 (1964); A. I. Larkin and Y. N. Ovchinnikov, *Zh. Eksp. Teor. Fiz.* **47**, 1136 (1964), [*Sov. Phys. JETP* **20**, 762 (1965)].
 - [13] Y. Yanase and M. Sigrist, *Journal of Physics: Condensed Matter* **23**, 094219 (2011).
 - [14] K. Miyake, *J Phys Soc Jpn* **77**, 123703 (2008).
 - [15] K. M. Suzuki, M. Ichioka, and K. Machida, *Phys. Rev. B* **83**, 140503 (2011).
 - [16] R. Ikeda, Y. Hatakeyama, and K. Aoyama, *Phys. Rev. B* **82**, 060510 (2010).
 - [17] Y. Kato, C. D. Batista, and I. Vekhter, *Phys. Rev. Lett.* **107**, 096401 (2011).
 - [18] G. D. Mahan, *Many-Particle Physics*, 3rd ed. (Plenum Publishers, 2000).
 - [19] A. Vorontsov and M. Graf, *Phys. Rev. B* **74**, 172504 (2006).
 - [20] W. A. Roshen and J. Ruvalds, *Phys. Rev. B* **28**, 1329 (1983).
 - [21] K. McElroy, R. W. Simmonds, J. E. Hoffman, D.-H. Lee, J. Orenstein, H. Eisaki, and S. Davis, *Nature* **422**, 592 (2003).
 - [22] M. P. Allan, F. Massee, D. K. Morr, J. V. Dyke, A. W. Rost, A. P. Mackenzie, C. Petrovic, and J. C. Davis, *Nature Physics* **9**, 468 (2013).
 - [23] T. Maehira, T. Hotta, K. Ueda, and A. Hasegawa, *J Phys Soc Jpn* **72**, 854 (2003).
 - [24] D. Hall, E. C. Palm, T. P. Murphy, S. W. Tozer, Z. Fisk, U. Alver, R. G. Goodrich, J. L. Sarrao, P. G. Pagliuso, and T. Ebihara, *Phys. Rev. B* **64**, 212508 (2001).
 - [25] C. Capan, Y.-J. Jo, L. Balicas, R. G. Goodrich, J. F. DiTusa, I. Vekhter, T. P. Murphy, A. D. Bianchi, L. D. Pham, J. Y. Cho, J. Y. Chan, D. P. Young, and Z. Fisk, *Phys. Rev. B* **82**, 035112 (2010).